Development of Oxide Growth Model for Cr-coated ATF and Microstructural Characterization on the Oxide Layer

Hyeongtak Kang, Dongju Kim, Youho Lee*
Department of Nuclear Eng., Seoul National Univ., 1 Gwanak-ro Gwanak-gu, Seoul 08826, Republic of Korea
**Corresponding author: leeyouho@snu.ac.kr*

***Keywords: Accident Tolerant Fuel (ATF), Cr coated cladding, Oxide growth, EBSD**

1. Introduction

Zirconium alloy has been used for cladding material in reactors for a long time. However, after the Fukushima Daiichi accident, there have been concerns about cladding oxidation and hydrogen generation by high temperature steam when a loss of coolant accident (LOCA) or a station black out (SBO) occurs. To solve these problems, an Accident Tolerant Fuel (ATF) concept has been developed [1]. The most prominent concept is chromium-coated Zircaloy because its mechanical and neutron economy features are similar to current Zircaloy cladding.

By applying chromium coating to the outer surface of the cladding, the oxidation during the steady state operation or accident conditions can be significantly reduced [2]. Still, it is important to estimate the oxidation kinetics of chromium coating since it affects the protection time of coating [3] and it can affect thermal properties (i.e., thermal resistance, heat transfer) of coating. In such a context, this study aims to develop a chromium oxide growth model for chromium-coated Zr-1.1Nb cladding.

In this study, the oxidation of chromium-coated Zr-1.1Nb cladding was conducted using thermogravimetric analysis (TGA) for various temperatures (1100-1300°C) and times. The chromium oxide thicknesses of post-oxidation specimens were measured using scanning electronic microscope (SEM) and image analysis. The parabolic oxide growth model was developed from the measured thickness data. The uneven thickness of the chromium oxide layer was observed and corresponding microstructure characterization using electron backscatter diffraction (EBSD) was carried out. In addition to that, the in-situ weight gain of the specimen was compared with weight gain by an oxide layer, and oxygen concentration in the Zircaloy matrix was measured by electron probe micro analysis (EPMA) analysis.

2. Experiment

2.1. Materials

Chromium coated Zircaloy cladding tubes were used in this research. The base material was Zr-1.1Nb alloy and the coating thickness was 16μm which was coated by Arc ion plating method. Each cladding tube had a 9.5 mm outer diameter, 0.57mm thickness and was cut into 8 mm lengths.

The cladding tube was sealed with a zirconia plug and sodium silicate cement to prevent inner oxidation of the Zircaloy, see Fig.1.

Fig. 1. Cladding tube sealed by plug and cement.

2.2. Methodology

The oxidation experiment was performed by TGA equipment from SETERAM. The sample was heated up to five different target temperatures (1100, 1150, 1200, 1250, 1300 °C) with a rate of 50℃/min. Then, the sample was exposed to isothermal steam oxidation for three or four target times. After the isothermal oxidation, the sample was cooled to room temperature at a rate of 50℃/min.

After the experiments, A MATLAB analysis of the SEM images was used to measure the thickness of each phase after oxidation.

The measurement process is shown in Fig.2. Fig.2 (a) and Fig.2 (b) are cross section images of the as-received sample and cladding which were conducted oxidation in 1200℃, 60min respectively. Using Fig.2 (b), the phase to be measured was separated from the other phases based on the brightness of the MATLAB images, as shown in Fig.2 (c). In this case, the oxide image was separated. Then the pixel counts were measured in a radial direction and converted into a length unit. The measured thickness of the phase is shown in Fig.2 (d).

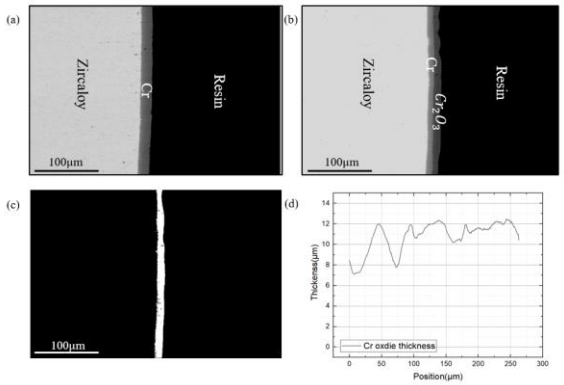

Fig. 2. (a) As-received cross section image of coated Zircaloy. (b) Cross section image after 60 minutes of oxidation at 1200℃. (c). Oxide divided image by MATLAB. (d) Measured thickness of oxide.

3. Result

3.1. Measured weight gain during the oxidation.

Fig. 3 shows weight gain data recorded by TGA. As can be seen, the weight gain rate increases with temperature. It showed parabolic-like weight gain for the early phase oxidation and there was a transition in weight gain under the extended exposure by protection loss of coating for the temperature range from 1150℃ to 1300℃. The experiment in this study was carried out in the parabolic growth region. However, in the case of 1100℃, protection loss was not observed until 18 hours.

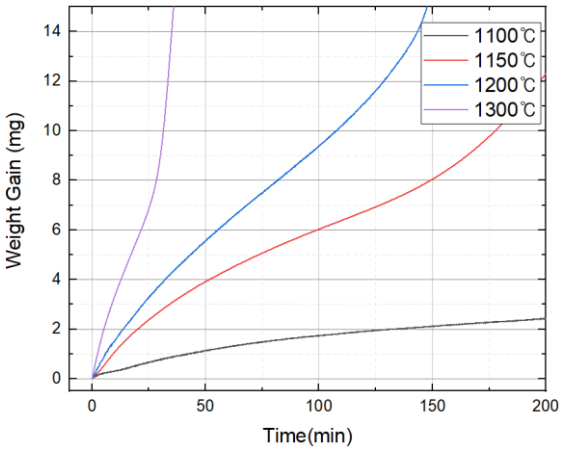

Fig. 3. Weight gain data over time.

3.2. Chromium oxide thickness

The oxide layer thickness was measured for all tested conditions. The result for specimen oxidized at 1200℃ was given for example in this paper. Fig 4 shows cross section image of cladding after oxidation at 1200℃. As shown in the figure, oxide thickness increases over time. It is noteworthy that chromium oxide layer had uneven thickness and interface unlike the Zircaloy oxide has a smooth oxide-metal interface.

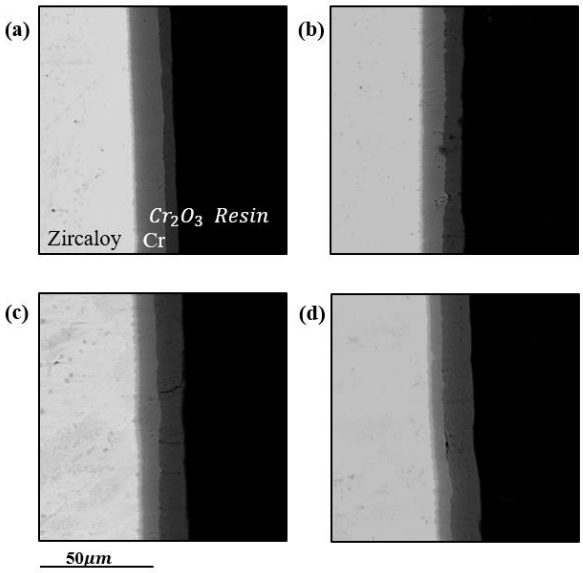

Fig. 4. Cross section image of 1200℃ oxidation sample images. (a) 10min. (b) 30min. (c) 60min. (d) 90min.

The measured distribution of oxide layer thickness shows the normal distribution with R square value of about 0.9 in every case, for most tested conditions. Fig. 5, shows the oxide thickness distribution corresponding to Fig. 4. The average oxide layer thickness increases over time and it has a significantly larger variation than the oxide layer of bare Zircaloy [4]. The average oxide layer thickness was used to develop a parabolic oxide growth model.

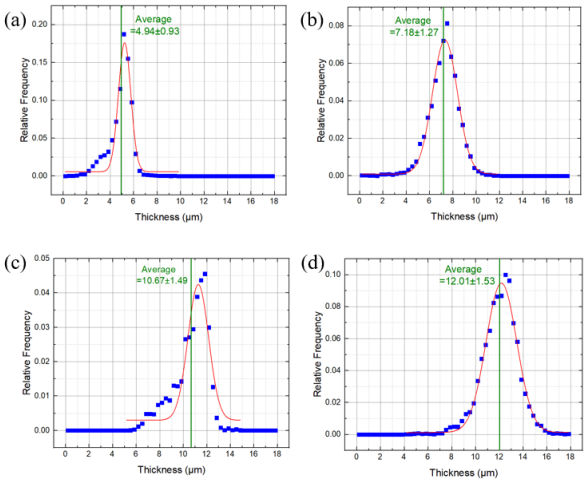

Fig. 5. Oxide layer thickness distribution and normal distribution fitting of specimen oxidized at 1200℃ (a) 10 min, (b) 30 min, (c) 60 min (d) 90 min.

3.3. Chromium oxide growth model

It is known that the oxidation rate follows a parabolic trend over time and that the oxidation constant (K_p) can be calculated using the Arrhenius equation [5]. According to Wagner theory, oxide thickness (δ) can be expressed as in Equations (2) and (3), where *t* is time, E_a

is activation energy, R is gas constant, and T is temperature.

$$(2)\ \delta = K_p\sqrt{t}\ [\mathrm{m}]$$
$$(3)\ K_p = k_0 \exp\left(-\frac{E_a}{RT}\right)\ \left[\frac{m}{s^{0.5}}\right]$$

In order to find the K_p, E_a, and k_0 values, linear and Arrhenius fitting was carried out. Since oxide thickness follows a normal distribution, the average thickness was used for fitting. The K_p value was obtained by linear fitting of the oxide thickness and the time squared. The fitting graph and obtained K_p values are shown in Fig. 6 and Table.2.

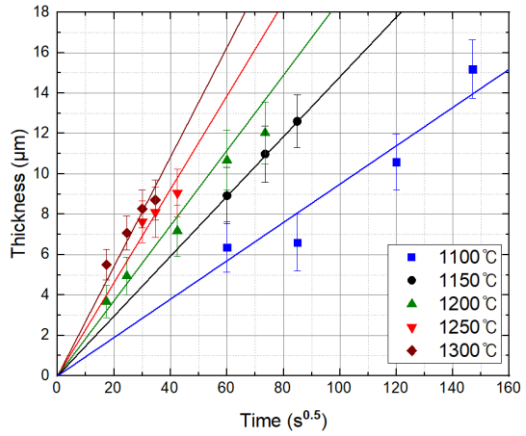

Fig. 6. Oxide thickness growth and linear fitting lines.

Table 2. K_p value based on temperature

Temperature (℃)	$K_p(\mathrm{m}/s^{0.5})$
1100	9.49E-08
1150	1.48E-07
1200	1.86E-07
1250	2.31E-07
1300	2.71E-07

E_a and k_0 values were obtained by fitting K_p and temperature in Equation 3. The results are shown in Fig.7 and each value is $5 \times 10^{-6}\left(\frac{m}{s^{0.5}}\right)$ and -98354 (J/K).

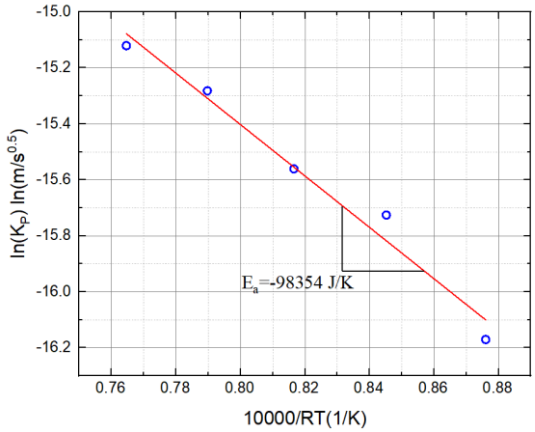

Fig.7. Arrhenius fitting of rate constant.

The developed model was validated using actual measurements. Comparing the predicted values from the developed model with the actual measurements, in most cases, they fall within an error range of 10% as shown in Fig. 8.

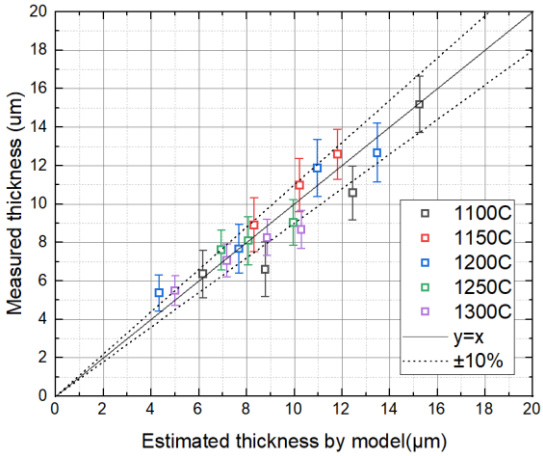

Fig.8. Validation of developed model by comparing expected value and measure value.

4. Discussion

4.1. Causes of uneven thickness

Uneven thicknesses and large deviations can be caused by various factors. There are two candidates for causes of uneven thickness. One is different oxidation rate depending on location and the other is high stress that can induce deformation of the layer.

The oxidation rate is governed by the diffusion rate of metal and oxygen. Since different microstructures can make different diffusion rates, microstructure and oxide thickness correlation analysis by EBSD was carried out. Chromium oxidation is governed by short circuit diffusion of chromium [5]. The most prominent candidate of short circuit diffusion is the grain boundary, and it can result in oxidation rate differences according to position and uneven thickness. So, an analysis of the misorientation of the grain boundary of oxide is carried

out. As shown in Fig. 9 (a)-(c), a comparison of the microstructure of each region with thick and thin oxide was conducted. Since the grain boundary of chromium oxide is the path of chromium and Oxygen, an analysis of the misorientation angle of oxide was conducted. As shown in Fig. 9 (d)-(f), there was no strong correlation between oxide thickness and misorientation angles.

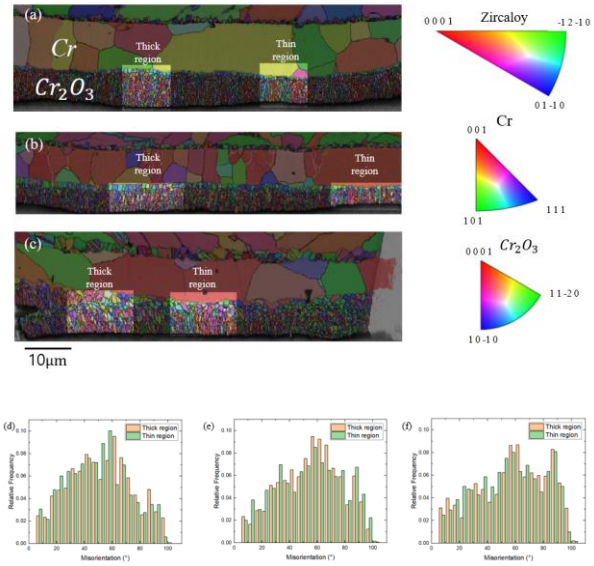

Fig. 9. EBSD map of coating oxide and misorientation angle within Cr oxide: (a)-(c) EBSD map of 1100℃, 120min, 1200℃, 10min , 1300℃, 10min , respectively. (d)-(f) misorientation angle distribution of (a)-(c), respectively.

Then, an analysis correlation between planar density of chromium and oxide thickness was conducted because of the possibility of atom number affecting oxidation rate. To check this out, the planar density of each Cr grain was calculated, and the thickness of the oxide which faces the Cr grain was measured. As shown in Fig 10, there was no correlation between planar density and oxide thickness. Also, as shown in Fig. 9 (a)-(c), uneven thickness is observed in the oxide which are facing the same Cr grain. As a result, there's no correlation between Planar density and oxide thickness.

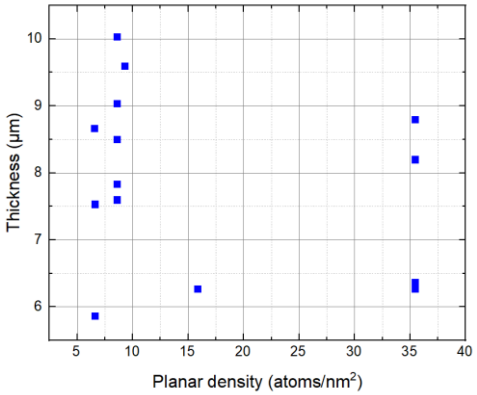

Fig. 10. Planar density and Oxide thickness of 1200℃ 60min oxidation specimen.

Another candidate is the stress effect of oxidation. Chromium has a large Pilling-Bedworth ratio (PBR) of 2.07. The high PBR causes large stress when metal is oxidizing, and it can lead to uneven oxide thickness. Another candidate is different chromium diffusion rates depending on position. Linked to the first reason (PBR), there is an argument that grain boundary diffusion causes stress and plastic deformation [6], and it causes uneven oxide. Also, pores and microchannels in the oxide can be a short circuit.

4.2. Weight grain and oxide growth rate

Fig. 11 shows weight gain data for the whole specimen and the oxide weight gain in the 1200 ℃ oxidation experiment. Total weight gain (TGA) represents weight gain data recorded on the TGA equipment. The weight gain by oxide was calculated by converting the measured oxide thickness and thickness model into oxygen mass.

It can be found that total weight gain was slightly higher than weight gain of oxide and the difference was larger for longer oxidation. To clarify the origin of that difference, the oxygen concentration in zircaloy was measured by EPMA and it is shown in Fig. 12. As can be seen, the oxygen concentration in the zircaloy matrix increases for a longer oxidation time. By adding the weight gain by oxide and zircaloy, it aligns well with the total weight gain measured by TGA.

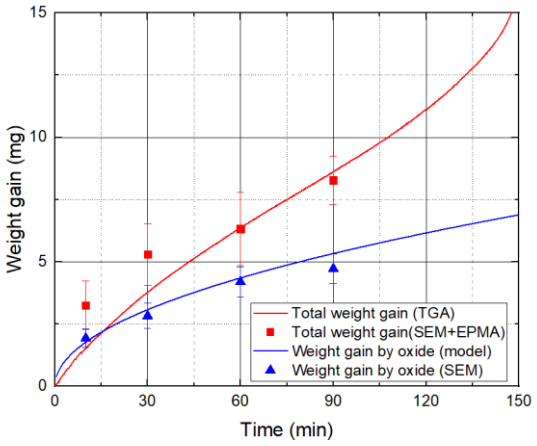

Fig. 11. Mass of whole specimen, oxide, and oxygen at 1200℃.

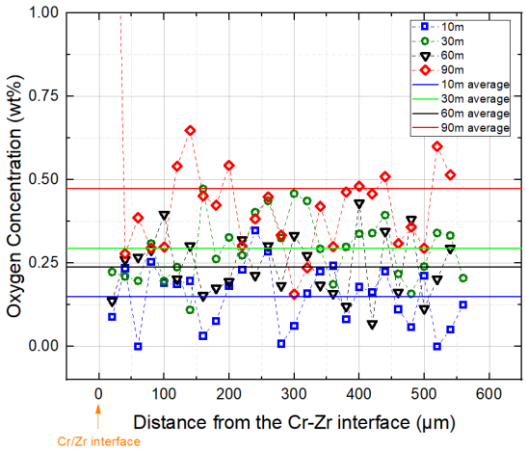

Fig. 12. Oxygen concentration in zircaloy of 1200℃ oxidation experiment measured by EPMA.

The EPMA mapping was conducted to analyze the cause of oxygen diffusion in the zircaloy matrix penetrating the coating. Fig. 13 shows the Zr mapping result of the specimen oxidized at 1200℃ for 1h. As can be seen in Fig. 13, a sharp Zr signal in the Cr coating was observed and some of the Zr signal had diffused up to the Cr/Cr_2O_3 boundary. This localized diffusion of zirconium through the coating and consequent partial loss of protectiveness would play an important role for the diffusion of oxygen in the zircaloy matrix.

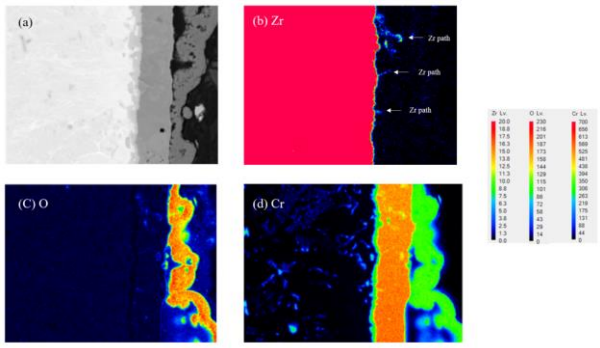

Fig. 13. EPMA mapping of specimen oxidized at 1200℃ for 60 min. (a). SEM image. (b) Zirconium. (c) Oxygen. (d) Chromium.

5. Conclusion

Experiments were conducted to develop an oxide growth model for Zr-Nb1.1 cladding with a chromium coating thickness of 16 μm. The oxidation behavior at various temperatures and oxidation times was measured, and based on the data, a parabolic oxidation growth model was developed. The developed model can predict the oxide layer thickness within an error of less than 10% for most cases. In addition, an uneven thickness of the chromium oxide layer was observed, and corresponding microstructural characterization was performed using electron backscatter diffraction (EBSD).

ACKNOWLEDGEMENT

This work was supported by Korea Institute of Energy Technology Evaluation and Planning (KETEP) grant funded by the Korea government (MOTIE) (No. 20224B10200100, Development of Commercialization Technology for Enhanced Accident Tolerant Fuel).

REFERENCES

[1] Terrani KA, Accident tolerant fuel cladding development: Promise, status, and challenges, Journal of Nuclear Materials, Vol. 501, pp. 13-30, 2018.
[2] Brachet, J.-C., Rouesne, E., Ribis, J., Guilbert, T., Urvoy, S., Nony, G., Toffolon-Masclet, C., Le Saux, M., Chaabane, N., & Palancher, H, High temperature steam oxidation of chromium-coated zirconium-based alloys: Kinetics and process, Corrosion Science, Vol, 167, pp. 108537, 2020.
[3] D. Kim, Y. Lee, Comprehensive Study on the Loss of Protectiveness Behavior in Cr-Coated ATF in High-Temperature Steam Oxidation, In Preparation.
[4] Ma, H.-B., Yan, J., Zhao, Y.-H., Liu, T., Ren, Q.-S., Liao, Y.-H., Zuo, J.-D., Liu, G., & Yao, M.-Y, Oxidation behavior of Cr-coated zirconium alloy cladding in high-temperature steam above 1200° C, Materials Degradation, Vol.5, pp. 7., 2021.
[5] Atkinson, A, Wagner theory and short circuit diffusion, SAGE Publications Sage UK: London, England, 1988.
[6] Kofstad, P, On the formation of porosity and microchannels in growing scales, Oxidation of Metals, Vol. 24, pp. 265-276, 1985.